NASA TECHNICAL MEMORANDUM

NASA TM X-71479

NASA TM X-71479

HIGH GAS VELOCITY BURNER TESTS ON SILICON CARBIDE AND SILICON NITRIDE AT 1200° C

by William A. Sanders and Hubert B. Probst
Lewis Research Center
Cleveland, Ohio 44135

TECHNICAL PAPER presented at Army Materials
Technology Conference on Ceramics for High Performance Applications
Hyannis, Massachusetts, November 13-16, 1973

HIGH GAS VELOCITY BURNER TESTS ON SILICON CARBIDE AND SILICON NITRIDE AT 1200° C

WILLIAM A. SANDERS and HUBERT B. PROBST
National Aeronautics and Space Administration
Lewis Research Center
Cleveland, Ohio

E-7798

ABSTRACT

Ten SiC materials and five Si_3N_4 materials were exposed in a Mach 1 gas velocity burner simulating a turbine engine environment. All materials studied are commercially available. Cyclic tests up to 100 hour duration were conducted at specimen temperatures of 1200° C. A specimen geometry was used that develops thermal stresses during thermal cycling in a manner similar to blades and vanes of a gas turbine engine. Materials were compared on a basis of weight change, dimensional reductions, metallography, fluorescent penetrant inspection, x-ray diffraction analyses, failure mode and general appearance. One hot pressed SiC, one reaction sintered SiC, and three hot pressed Si_3N_4 materials survived the program goal of 100 1-hour cycle exposures. Of the materials that failed to meet the program goal, thermal fatigue was identified as the exclusive failure mode.

INTRODUCTION

SiC and Si_3N_4 have been identified in several recent investigations (Refs. 1-11) as outstanding candidates for advanced turbine engine vane and blade applications. Notable among these investigations is a five-year iterative design and materials development program initiated in July 1971 by the Advanced Research Projects Agency (Refs. 3, 7, 10).

The goal of this program is to demonstrate successful use of brittle materials in two land based gas turbine applications: a small vehicular gas turbine engine and a large stationary gas turbine for electric power generation.

This current interest in non-metallic materials for gas turbine applications arises primarily from the inability of classical superalloys to meet the demands of advanced engines. As discussed in Lewis Research Center work (Ref. 1) the best coated and cooled nickel- and cobalt-base superalloys for aircraft engine application are limited by corrosive attack to a material temperature of about 1100° C. Improved aircraft performance and economy require higher turbine inlet gas temperatures with turbine material temperatures exceeding 1100° C. In reference 1 the merits of refractory compounds for advanced turbine application are also discussed. In burner rig tests on rod-shaped specimens, high density forms of SiC and Si_3N_4 proved to be outstanding among the 20 other non-metallic refractory materials. In that investigation testing was conducted at a material temperature of 1204° C in a high gas velocity burner rig simulating a turbine engine environment. The dense SiC and Si_3N_4 materials met the program goal of 120 cycles (total time at temperature of 10 hours) at 1204° C in a Mach 1 hot gas stream, and showed no signs of cracking or surface degradation and only slight changes in weight. Other materials in the Lewis study which showed some promise for turbine use were lower density forms of SiC and Si_3N_4, a SiC composite containing silicon and carbon, and chemical vapor deposited (CVD) SiC.

The purpose of the present investigation was to further evaluate and compare several commercial varieties of SiC and Si_3N_4 in a Mach 1 burner simulating an engine environment. In this study a more realistic specimen geometry was used which incorporated a simulated leading edge of an airfoil. This geometry allowed the material to encounter severe thermal stresses more closely approximating a real engine vane than did the cylindrical specimen of the previous screening study (Ref. 1).

The burner used for this evaluation was operated at a hot gas velocity of Mach 1 with Jet A, a kerosene-type fuel similar to JP5 fuel. Each material was cyclically heated to a temperature of 1200° C in the burner hot gas stream. Maximum target exposures for this program consisted of 100 one-hour cycles (100 hours total time at temperature). Various types of SiC and Si_3N_4 were evaluated and compared on the basis of weight change, dimensional loss, pre- and post-test metallography, fluorescent penetrant inspection, x-ray diffraction analysis, failure mode, and general appearance. A commercially coated thoria dispersed 80 nickel-20 chromium alloy (TD-NiCr) was also included in the program for comparative purposes. This alloy has sufficient strength at 1200° C for some low stress turbine applications.

MATERIALS

Table I lists and categorizes the 15 ceramic materials evaluated. Given in the table are the material vendors, general fabrication method, shape provided, purity, and some physical and mechanical properties. In all cases except two, specimens were cut from billets and ground to

final dimensions at Lewis. One exception was reaction sintered Si_3N_4 which was produced in specimen form by Norton Company. The other was chemical vapor deposited (CVD) SiC specimens which were supplied by Energy Research Corporation already machined to shape from individual CVD billets. Not listed in table I is the commercially coated 80 $^{w}/_{o}$ Ni-20 $^{w}/_{o}$ Cr alloy containing 2 $^{w}/_{o}$ thoria for dispersion strengthening. The coating was an oxidation resistant aluminide resulting from a duplex process involving first chromium diffusion and then aluminide formation.

The ceramic material fabrication methods and consolidation techniques generally employed by producers are as follows:

Hot pressed silicon carbide. - For the hot pressed SiC materials, a -325 mesh SiC powder is blended with small amounts of alumina, iron oxide or boron which act as densification aids. The SiC powder and additive(s) are sometimes milled in tungsten carbide mills to obtain a finer particle size and a more intimate mixture of SiC and densification additive. After blending or milling, the SiC powder is hot pressed in graphite dies to produce nearly 100% dense billets. Typical hot pressing conditions are: temperature, 2150° C; pressure, 27.5 MN/m^2; and time, 60 to 120 minutes.

Reaction sintered silicon carbide. - Although the term reaction sintered SiC is used to describe five SiC-base materials, the Norton low-fired and high-fired materials are more correctly referred to as recrystallized silicon carbides (Ref. 2). These two materials are made by firing slip cast bodies of crushed and milled SiC powder of bimodal particle size distribution. Firing temperatures of 2100 to 2500° C result in self-bonded SiC bodies of about 18% porosity. Two of the

remaining three materials in this second category result from the molten silicon infiltration of a porous SiC-C body and a carbon fiber preform. Reaction between the molten silicon and carbon in the SiC-C body results in the formation of more SiC and a final body fully dense consisting of SiC and free Si-(Refel) (Ref. 12). Reaction of the molten silicon with the carbon fiber preform results in a 3-phase body consisting of SiC and unreacted C and Si (Ref. 13). The material, KT, is a two-phase, high density material of SiC and free Si and is described as characterized by a continuous, interlocking structure of SiC-bonded SiC (Ref. 14).

Chemical vapor deposited silicon carbide. - CVD SiC material is commonly produced by pyrolyzing a chlorosilane where carbon and silicon are supplied in the same molecule. Silicon carbide deposits result when gaseous chlorosilane and a hydrogen stream react to form SiC on a heated graphite substrate (Ref. 15). The substrate can then be removed by oxidation or machining to obtain a solid monolithic CVD SiC shape.

Hot pressed silicon nitride. - The hot pressed silicon nitride material is prepared in essentially the same manner as is hot pressed SiC. Alpha phase Si_3N_4 powder, -325 mesh, is blended with small amounts of magnesium oxide (MgO) which acts as a densification aid. The Si_3N_4 powder may be milled with the MgO additive in tungsten carbide mills to obtain a finer particle size and a better mix of Si_3N_4 powder and MgO additive. The consolidation of the Si_3N_4 powder to nearly 100% dense billets is then effected by hot pressing in graphite dies at these typical conditions: temperature, 1750° C; pressure, 27.5 MN/m^2; and time, 60 to 120 minutes.

Reaction sintered silicon nitride. - The reaction sintered silicon nitrides which are often referred to as "reaction bonded" result from the nitridation in the green state of silicon powder compacts from a variety of consolidation methods such as die pressing, slip casting, extrusion, isostatic pressing, flame spraying, and injection molding. If a binder is used, this is removed by heating at about 400° C. This is followed by heating at 1200° C in a nitrogen atmosphere to effect a partial nitridation. In this partially nitrided state the part can be machined with conventional tooling to final dimensions. A final nitriding at 1400° C completes the nitriding process with negligible dimensional changes. Firing times are dependent on section thickness, with a 50-hour firing time being a norm. Densities of 75 to 80% of theoretical are typical for reaction sintered Si_3N_4.

SPECIMENS AND APPARATUS

Specimen geometry. - The specimen geometry and dimensions are shown in figure 1. One long edge (hereafter referred to as the leading edge) of the simulated blade specimen tapers as is shown in figure 1 to a radius of approximately 0.08 cm (0.03 in.). In test, the hot gas stream impinges directly on this leading edge. The tapered leading edge constrained by the more massive (and slower thermal response) body of the specimen leads to thermal stresses during thermal cycling. The groove and notch near the base of the test specimen provide a means for locking the specimen in place in the burner rig holder. Due to process limitations on deposition thickness, the CVD SiC specimens were only 0.32 cm (0.13 in.) thick instead of the standard thickness of 0.64 cm (0.25 in.) indicated in figure 1.

Burner rig. - A schematic of the burner rig described in detail in reference 16 is shown in figure 2. The apparatus was operated with Jet A fuel at a combustion gas velocity of Mach 1 at the conditions given in table II. To attain the 1200° C material test temperature, the required burner gas temperature was approximately 1540° C, which for Mach 1 conditions resulted in a nozzle exit gas velocity of 850 mps (2800 fps). Specimens were tested singly with the leading edge facing the burner nozzle as shown in figure 3. Metal specimens on each side of the ceramic specimen acted as radiators in order to augment the heat input to the specimen.

Specimen retention method. - Test specimens were held in the holder primarily by a pin-lock bolt method as shown in figure 3. An additional specimen retention method used along with the pin-lock bolt method was a side bolt which bore against a flat, loose plug loading the specimen in compression from the side as shown in figure 3. A third retaining device, also shown in figure 3, was a short specimen retainer rod which bore against the lowest portion of the specimen leading edge. Both bolts and the retainer rod were fixed in position by safety wires under tension.

PROCEDURE

Temperature. - For temperature calibration prior to tests, an internally thermocoupled nickel-base superalloy specimen was used. During tests, the temperature of the specimen being tested was monitored with an optical pyrometer. Approximately the same burner operating conditions established for the calibration temperature of 1200° C on the superalloy specimen were used for all test materials. All materials were observed

to reach the 1200° C hot zone test temperature within 30 seconds of exposure. With the hot zone flat portions of the test specimens held at 1200° C it was found that the leading edge ran at a temperature of 1240° C. The burner gas temperature was automatically controlled by a total radiation pyrometer which was focused on the test specimen. At test temperature, all specimens exhibited uniform hot zones for a distance of approximately 1.9 cm (0.75 in.) above and below the centerline of the burner nozzle. Within this zone the 1200° C test temperature was maintained within ±8° C.

Exposure cycle. - The exposure goal for the test materials was 100 cycles. A cycle consisted of one hour at the 1200° C test temperature followed by a 5-minute still air cool effected by rapid lowering of the test specimens out of the hot gas stream. In the cooling portion of the cycle, the specimen cooled to black heat within 30 seconds and to near room temperature within the 5 minute cooling period. Duplicate tests were run on most materials which survived 100 cycles. In the event of a failure in less than 20 cycles, i.e., prior to the first inspection, the material was retested in some instances as many as seven times to establish the failure mode and the number of cycles to failure.

Inspection. - Dense specimens were inspected in the as-received condition under black light after treatment with a penetrating oil, an emulsifier, and powder developer. After this inspection, all dense specimens were degreased in trichlorethylene, weighed to ±0.2 mg and individually wrapped for storage until test exposure. As-received porous materials were examined for surface damage with a 30 X binocular microscope, dried in an oven, weighed to ±0.2 mg and individually wrapped

for storage until use. The high porosity precluded the use of the oil penetrant crack inspection method. Before testing each specimen was measured for breadth and thickness with a micrometer with a precision of 1 micrometer (micron). Measurements were made at the center of the intended hot zone which was also the metallographic sectioning plane as indicated in figure 1.

Test specimens were removed from the burner rig after every 20 cycles for inspection. Inspection consisted of weighing, photographing, and determining if thermal fatigue cracking had occurred. Inspection for cracks was by fluorescent penetrant for dense materials and by means of a 30 X binocular microscope for porous materials.

For comparison with the initial dimensions, the breadth and width of polished cross sections of those test specimens which survived 100 cycles plus a few others were measured using an optical micrometer having a precision of 1 micrometer. Previous experience has indicated that optical micrometer measurements on untested polished test specimens cross sections agree within 1 micrometer with micrometer measurements made on the untested specimens before sectioning.

Metallographic examination. - Hot zone surfaces of those specimens which survived 100 cycles and of salvaged pieces of a few failed specimens were subjected to in situ x-ray diffraction analysis. These were then mounted in epoxy resin, sectioned through the hot zone as shown in figure 1 and polished and etched for metallographic analysis. For SiC a two-step etch consisting of concentrated HF followed by 10% chromic acid solution was generally effective. In a few cases a 700-800° C molten mixture of 30 $^{w}/_{o}$ NaF and 70 $^{w}/_{o}$ $NaCO_3$ was necessary to delineate

grain boundaries. For all Si_3N_4 materials a boiling etchant consisting of 6 parts HF, 5 parts H_2O_2 and 2 parts HNO_3 was required to reveal the microstructure. All SiC and Si_3N_4 materials were also examined metallographically in the as-received condition. The light microscope, the electron microscope and the scanning electron microscope were all used to examine the polished and or etched sections.

RESULTS AND DISCUSSION

The detailed behavior of the SiC and Si_3N_4 materials will be discussed in the order of the material categories given in table I. The following general observations refer to all test materials. The results consist of weight change data, fluorescent penetrant, and microscope examination for cracks, dimensional loss data, metallography, x-ray diffraction data, failure mode, and general appearance of the specimens. In contrast to the results in reference 1 where three predominant failure modes, mechanical failure due to gas loading, thermal shock, and thermal fatigue were all prevalent in the burner rig testing of non-metallic rod shaped specimens, only one clear failure mode, thermal fatigue, predominated in the present work on SiC and Si_3N_4 simulated blade shapes. The thermal fatigue failure is defined as specimen failure in the hot zone during cyclic exposure after surviving for at least one cycle, a cycle consisting of a 1-hour exposure at 1200° C in the hot gas stream, followed by a 5-minute still air cool. A summary of test results is given in table III and a summary of specific weight change and dimensional loss data is given in table IV. Breadth dimension losses are in all cases greater than thickness dimension losses since the leading edge runs slightly hotter than the side of the sample and

because of its geometry is more vulnerable to attack. A plot of specific weight change versus exposure cycles for SiC and Si_3N_4 materials which survived 20 or more cycles is given in figure 4. The curves of figure 4 are drawn through actual data points since the number of samples tested of any given material were insufficient to allow averaging of the data. In cases where two samples were run the curve plotted in figure 4 represents the "most well behaved" sample. That is, a specimen that was fairly free of abrupt weight changes that were obviously due to chipping in the base during exposure due to the specimen loosening slightly in the holder as will be discussed next.

As noted in table III, a frequent reason for cessation of test was failure of the specimen in the pin groove region of the specimen which is inside the stationary holder (see figure 3). Although great care was taken in specimen installation to avoid overtightening, to install every one in the same manner, and to check for tightness during 20 cycle exposure intervals, certain materials (generally those of lower strength) seemed prone to pin groove failure. This type of failure is felt to be due to an unavoidable (at least in these tests) occurrence, namely the specimen becoming slightly loose in the holder at some point during test. On some subsequent insertion into the hot gas stream the loosened specimen fails mechanically in the pin groove depending upon the material strength. The loosening is likely related to the fact that the steel holder coefficient of thermal expansion is approximately 3 times that of SiC or Si_3N_4.

HOT PRESSED SiC

In this category, only the Norton hot pressed SiC was able to attain the 100 cycle exposure goal. The other three hot pressed SiC materials failed in thermal fatigue as detailed in table III. Fluorescent penetrant inspection showed the Norton SiC specimen to be crack-free. As indicated in table IV and figure 4(a) a very slight specific weight gain was sustained by Norton hot pressed SiC. The limited data for the A.C.E. and Avco hot pressed silicon carbides indicate that these materials initially oxidize at a somewhat greater rate. Very slight dimensional losses of 14 and 4 micrometers were measured for Norton hot pressed SiC hot zone breadth and thickness dimensions. These losses represent an approximate reduction in load bearing area of only about 0.1%. Photographs of four hot pressed SiC specimens after test are shown in figure 5. The A.C.E., Avco, and Ceradyne stubs shown are the remnants of the longest lived specimens of those materials tested and are representative of the other hot pressed SiC specimens that failed in thermal fatigue. Hot zone surface x-ray diffraction analyses on the four specimens shown in figure 5 all indicated the presence of alpha-SiC (α-SiC) and alpha cristobalite (α-SiO_2).

Microstructures of the as-received hot pressed SiC materials are shown in figure 6. The Norton material was equiaxed and had a grain size of about 2 micrometers and a rather homogeneously dispersed dark etching constituent. The A.C.E. SiC material also had equiaxed grains but the grains were larger with a size of about 5 micrometers. Dark areas, either porosity and/or pull-outs are evident in the A.C.E. material. Both the Avco and Ceradyne SiC materials had microstructures

consisting of tabular grains. The Avco SiC material was coarser grained than the Ceradyne by a factor of two, typically 14 micrometer x 40 micrometer tabular grains for Avco and 7 micrometer x 20 micrometer tabular grains for Ceradyne. Avco and Ceradyne microstructures also exhibit fairly large pores compared to either A.C.E. or Norton. The light etching phase apparent in Avco and Ceradyne are probably associated with the use of densification aides. The Norton SiC as-received microstructure is also shown by electron micrography in figure 7. Here the dark etching areas shown in figure 6 have the same shade and texture as the larger grains, however, they appear to be comprised of clusters of small grains with individual grain diameters usually less than 1 micrometer. Thus the "dark etching" areas of figure 6 would appear to be ultra fine grained SiC appearing dark because of the heavily etched grain boundaries, rather than being a separate phase.

The Norton hot pressed SiC specimen which survived 100 cycles of exposure was sectioned and polished for post-test metallography; a scanning electron micrograph of this Norton specimen is shown in figure 8. An adherent continuous α-SiO_2 layer of about 3 micrometers thickness was found to cover the specimen in the hot zone. The continuity of this layer indicates that it should afford good protection against further oxidation of the SiC.

Thus, long life in the burner rig for hot pressed SiC is favored by high density and small grain size. In addition to small grain size per se, the duplex grain size in the Norton material could play an important role in resisting thermal fatigue. The larger grained materials, Avco

and Ceradyne, in addition to inferior lives also exhibited a wide variability in behavior with Avco SiC giving lives of from 1 to 47 cycles.

REACTION SINTERED SiC

Five SiC-base materials are included in this category for convenience, but as described in the materials section the Norton low-fired and high-fired materials might be more accurately described as "recrystallized silicon carbides" while the Refel, KT, and Si-SiC-C materials more properly fit the "reaction sintered SiC" designation. But even with these three materials as discussed in the materials section, there are distinctions in the fabrication methods.

Refel SiC was the only material of the reaction sintered category which survived 100 cycles of exposure without damage. X-ray analysis of the Refel SiC specimen showed α-SiC, Si, and α-SiO_2. The Norton low-fired and high-fired SiC materials and the Carborundum KT SiC exhibited thermal fatigue failures as listed in table III. A Norton low-fired SiC specimen also failed at the pin groove due to loosening in the holder--a test result which was described and discussed at the beginning of the Results and Discussion section. The last material in the group, the Si-SiC-C material, could not survive more than 1 cycle due to oxidation of the carbon phase at the surface. Due to the removal of carbon from the leading edge of the Si-SiC-C specimen, deep grooves formed which resulted in mechanical failure in the second cycle.

The specific weight change data for Refel SiC are given in table IV and plotted in figure 4(b). The oxidation behavior of the Refel material was very similar to the behavior of Norton hot pressed SiC plotted in figure 4(a). No dimensional loss in thickness was noted for the Refel SiC

but a 17 micrometer loss in breadth was measured, similar to the 14 micrometer loss for the Norton hot pressed SiC.

The only other specific weight change data obtained for the reaction sintered SiC group was an extremely high 20 cycle specific weight increase of 17.4 mg/cm^2 (table IV) for the Norton low-fired SiC material. This great weight increase--over 2 orders of magnitude greater than that of Refel SiC--attests to the open structure (18% porosity) and great surface area for oxidation of the Norton low-fired SiC.

Photographs of three reaction sintered SiC specimens after test are shown in figure 9. The Refel SiC after 100 cycles shows no damage while thermal fatigue cracks were found by fluorescent penetrant inspection of KT SiC after 10 cycles exposure. This specimen was not tested further but would be expected to fail at an existing crack on next insertion into the hot gas stream. This KT SiC specimen was not cracked after 5 cycles. The 20 cycle condition of the Norton low-fired SiC specimen is shown in the third photograph in figure 9. In this photograph the heavy oxidation of Norton low-fired SiC previously noted by great weight gain is evidenced by very prominent silica flow lines in the hot zone.

As-received microstructures of the five reaction sintered SiC materials are shown in figures 10 and 11. The Refel SiC in figure 10 is a very homogeneous material with 9 micrometer equiaxed SiC grains and a uniform dispersion of free Si. KT SiC is a much less homogeneous material characterized by a wide range of grain sizes and large islands of free Si. The Si-SiC-C material has a striated structure which one would expect since the material results from the molten silicon infiltration of a carbon fiber preform. In the Si-SiC-C microstructure the

dark stringers are unreacted carbon, the light gray material is SiC and the white material is free Si. These three phases were identified by x-ray diffraction. In figure 11 the Norton low-fired and high-fired SiC materials can be compared. Both materials are prepared in the same way up to the point of firing a slip cast compact of bimodal powder particle size distribution. In the low-fired SiC, a duplex grain structure with very fine porosity is clearly evident. As a result of higher firing temperature the high-fired SiC microstructure appears as a material in the process of grain growth--the large grains growing by surface bonding with small grain clusters but with the formation of large pores.

The Refel SiC specimen which survived 100 cycles was sectioned through the hot zone for post test metallography. A light micrograph of the Refel SiC is shown in figure 12, and a slightly rough but continuous layer of α-SiO_2 about 5 micrometers thick can be noted.

The comparison of behavior and microstructures of Refel and KT illustrate the importance of microconstituent distribution. Although both materials are fully dense and both contain about 10% free silicon the burner rig behavior of Refel is far superior. As shown in figure 10, the fine grain structure and homogeneous distribution of free silicon are in obvious contrast to the much larger grain size and inhomogeneous distribution of silicon in KT.

The behavior of the Norton low-fired and high-fired SiC materials again illustrates the importance of homogeneity and flaw size. While neither material was judged satisfactory, the low-fired SiC did exceed 20 cycles while the high-fired SiC could survive only one cycle. Both materials have similar densities but the distribution of the porosity

obviously accounts for the differing behavior. In the low-fired material the porosity is evenly distributed generally as small pores while the high firing has resulted in more complete sintering of the fine grained constituent giving larger pore sizes as is evident in figure 11.

Refel and hot pressed Norton SiC behaved quite similarly in that both met the goal of 100 cycles and both exhibited similar weight and dimensional changes. This suggests that the 10% free silicon in Refel has not altered the ability of SiC to sustain thermal cycling nor has it degraded oxidation resistance of SiC under these test conditions at 1200° C.

CHEMICAL VAPOR DEPOSITED (CVD) SiC

In this category only one material was tested; half thickness specimens were supplied in test shape by Energy Research Corporation. As noted in table III, CVD SiC specimens were difficult to hold in test and failed 4 times due to loosening in the holder. A superalloy shim was used to center each half-thickness CVD SiC specimen in the burner rig holder and the additional interface resulting is felt to have aggravated a loosening tendency always present. A maximum exposure of 52 cycles was obtained on one specimen and fluorescent penetrant inspection showed the hot zone to be crack-free. Only a 20 cycle specific weight gain data point was obtained for this CVD SiC specimen. Weight gain was slight, the same as that for hot pressed Norton SiC. Dimensional loss for the CVD SiC specimen exposed for 52 cycles was slight as given in table IV, 5 micrometers on breadth and 3 micrometers on thickness. This results in a reduction of load bearing area less than 0.1%. The

52 cycle exposure CVD SiC specimen is shown in figure 13(a). The failure may have originated at the corner of the base notch. Shown in figure 13(b) is the fracture cross section showing the columnar structure characteristic of CVD SiC. Microstructures in the plane of deposition and in the plane perpendicular to the deposition plane are shown in figures 13(c) and 13(d) respectively. The characteristic columnar grain structure of the CVD SiC material is again apparent in figure 13(d). A typical columnar grain was approximately 8 micrometers x 27 micrometers. Hot zone surface x-ray diffraction analysis on the 52 cycle sample showed β-SiC and α-SiO_2. No α-SiO_2 layer could be observed on a polished hot zone cross section of the 52 cycle CVD SiC specimen. On the basis of these results for CVD SiC and keeping in mind its attractive properties (Ref. 15) of essentially no porosity, high purity and high strength, it is felt that CVD SiC specimens if properly held could easily survive 100 cycle exposure.

HOT PRESSED Si_3N_4

All three hot pressed Si_3N_4 materials were exposed for the full 100 cycle planned exposure without sustaining damage as shown in figure 14(a). Zyglo inspection did not reveal any cracks. The weight changes given in table IV and plotted in figure 4(c) show the Ceradyne and Avco materials behave similarly with both materials gaining weight up to 60 cycles and losing weight beyond 60 cycles. The Norton Si_3N_4 material (HS-130) displayed a somewhat different behavior, gaining less weight up to 20 cycles but thereafter exhibiting a continually increasing weight loss out to 100 cycles. It has been reported in reference 7 that the static oxidation of hot pressed Si_3N_4 less pure in regards to

such elements as Ca and Al results in greater oxidation weight gains. Although impurity levels are not known for all three hot pressed Si_3N_4 materials it is known that Norton synthesizes their own starting powder while both Avco and Ceradyne use a high-alpha Si_3N_4 powder supplied by Advanced Materials Engineering of Great Britain. Thus it is possible that the more rapid oxidation of Avco and Ceradyne materials compared to Norton's is a reflection of purity difference even though x-ray diffraction analysis of the as-received samples revealed all were β-Si_3N_4. The high alpha Si_3N_4 content of starting powders has obviously converted to β phase as is common for hot pressed Si_3N_4 (Ref. 17).

Other similarities in the behavior of the Ceradyne and Avco materials and contrasts with the Norton material are exemplified by the dimensional losses given in table IV, and the occurrence of silica flow lines as shown in figure 14(b). Breadth and thickness losses for the Norton Si_3N_4 specimen were both only 3 micrometers while greater losses of 25 and 12 micrometers and 20 and 7 micrometers were sustained by the Ceradyne and Avco materials respectively. These dimensional losses translate into slight load bearing area reductions of approximately 0.06%, 0.3%, and 0.2% for the Norton, Ceradyne and Avco Si_3N_4 specimens respectively. As shown in figure 14(b) silica flow lines were noted after 100 cycles exposure on the hot zone leading edges of both Ceradyne and Avco specimens but no flow lines were observed on the Norton sample. Hot zone surface x-ray diffraction results were the same however, with all three showing the presence of β-Si_3N_4 and α-SiO_2. The presence or absence of SiO_2 flow lines could also be the result of purity

differences. The SiO_2 formed on a less pure Si_3N_4 could contain impurities and thereby be of lower viscosity and allow the obvious flow that has occurred in the high velocity gas stream.

Contrasts and similarities are again evident in the scanning electron micrographs of Si_3N_4 specimen polished hot zone cross sections given in figure 15. Here, the Norton material behavior differs from that of the Ceradyne and Avco materials which behaved much the same and are represented by a single electron micrograph of the Avco material. The silica layer on the Norton Si_3N_4 specimen was approximately 5 micrometers in thickness, while a thicker silica layer of about 18 micrometers thickness was the characteristic of both the Ceradyne and Avco materials. Again, these oxide layer thickness differences are reconcilable with the supposition that the Norton material is more pure and therefore oxidizes more slowly.

As evident in figure 4 the slope of the weight change versus time curves for all three hot pressed Si_3N_4 materials changed from positive to negative at some point within the 100 hour exposures. The weight loss could be the result of viscous flow and loss of some of the SiO_2 layer. The differences among the three materials regarding weight change curves and scale thicknesses after 100 hours reflect the net result of unknown but differing scale formation rates and scale loss rates.

The microstructure of all three hot pressed Si_3N_4 materials was very similar consisting of both equiaxed and tabular grains in the 0.5 to 2 micrometer grain size range. This microstructure is exemplified by the electron micrograph of the Norton Si_3N_4 shown in figure 16.

Thus, the hot pressed Si_3N_4 materials all performed admirably in burner rig testing. On the basis of the very slight weight changes alone it is not possible to rank one material over another. However, when the net result of SiO_2 scale formation and SiO_2 loss by viscous flow is considered it would appear that the Norton hot pressed Si_3N_4 may offer an advantage for long life applications. The controlling property here would be the level of impurities in powders for hot pressing and the effect of these impurities on the nature of the SiO_2 layer formed.

The eventual weight loss experienced by hot pressed Si_3N_4 contrasted to the continuing weight gain of SiC materials that survived 100 cycles must also be due to differences in viscosities of the SiO_2 scales formed on the two materials. Under static conditions in the absence of the surface shearing forces brought about by the high velocity gas, both materials continue to gain weight: Si_3N_4 (Ref. 7), SiC (Ref. 10). There was never any indication found that the SiO_2 scales were cracking and spalling due to the thermal cycling thus the weight losses are attributed to viscous flow.

REACTION SINTERED Si_3N_4

Two types of reaction sintered Si_3N_4 are compared in this section. Norton material (NC-350) as stated previously, was obtained in test specimen form while the A.M.E. specimens were machined from 1 cm (0.4 in) thick billets. Neither material reached the goal of 100 cycles as detailed in table III. Most failures resulted from the specimens failing mechanically in the pin groove due to loosening in the holder. However, on two occasions the A.M.E. material failed in thermal fatigue after 9 and 24 cycles.

The oxidation behavior of samples of these two materials was considerably different as indicated by the specific weight changes given in table IV and plotted in figure 4(d). The Norton material gained weight at a very rapid rate to at least 80 cycles while the limited data for the A.M.E. material shows only a very slight weight gain in the 20 to 40 cycle interval. At 40 cycles, the Norton material had almost 10 times the weight gain of the A.M.E. material. The Norton 92 cycle specimen lost 11 micrometers in thickness. Damage to the salvaged hot zone section of the Norton sample precluded a determination of breadth loss. Due to damage, no dimensional measurements were possible on the A.M.E. material. Photos of the Norton and A.M.E. specimens after 80 cycle and 40 cycle respective exposures are shown in figure 17(a). These specimens subsequently failed because of loosening in the holder after 92 cycles (Norton) and 49 cycles (A.M.E.). Figure 17(b) shows SiO_2 flow lines noted on the A.M.E. hot zone leading edge at the 20 cycle mark. No flow lines were noted on the Norton specimen through 80 cycle exposure. X-ray diffraction analyses from the surfaces of salvaged specimen hot zones indicated the presence of α-Si_3N_4, β-Si_3N_4 and α-SiO_2 for the Norton specimen after 92 cycles and the A.M.E. specimen after 49 cycles.

Microstructurally, the two as received reaction sintered Si_3N_4 materials were similar as shown in figure 18(a). Etched microstructures of the Norton material could not be obtained due to severe attack by the boiling HF-H_2O_2-HNO_3 etchant. For this reason, the figure 18(a) microstructures are in the as-polished condition. The A.M.E. material was more amenable to etching and figure 18(b) is a scanning electron

micrograph of an etched sample with a grain size less than 1 micrometer and an inhomogeneous distribution of voids.

It is believed that the unusually high oxidation rate observed for Norton material (fig. 4) is not truely representative of reaction sintered materials but rather is the result of the reaction sintering procedure used. This belief is based primarily on appearance of the samples, and microstructural observations as summarized below.

As-received Norton specimens (reaction sintered to shape) presented varying surface colors. One major side of the specimens was gray while all other surfaces including ends and leading edge taper were white. X-ray analysis of the white and gray surfaces revealed only α-Si_3N_4 and β-Si_3N_4. Judging from x-ray diffraction line intensities both sides exhibited an α phase to β phase ratio of about 4 to 1. In no case was any unreacted silicon identified. Microstructures after exposure revealed gross differences in oxidation behavior of the two sides of Norton specimens as illustrated in figure 19. The gray side reveals a uniform and continuous layer of SiO_2 scale. In contrast the white side has been more severely attacked showing deep and irregular pockets of SiO_2 formation. It appears obvious that the high weight gains recorded for the Norton material are due to the gross attack that occurred on the white side of specimen. The basic cause of the differing characteristics of the two sides of the Norton specimen is no doubt due to some differences in the environmental and positional conditions to which the two sides were exposed during nitriding. It is presumed that the process could be adjusted so that an entire specimen would oxidize at the lower rate.

By comparison the A.M.E. reaction sintered material was machined from a completely nitrided slab (table I) so that any locally varying surface conditions during nitriding would not be expected to affect behavior of the machined specimen. Thus, the as-received A.M.E. specimens appeared gray and x-ray analysis indicated an alpha phase to beta phase ratio similar to that of the Norton specimens. The weight gain of A.M.E. specimen was correspondingly less (fig. 4) and the microstructure of exposed specimen was identical to that of the gray side of Norton specimen (fig. 19). Thus, it is concluded that the oxidation behavior of A.M.E. material is a truer measure of the behavior of reaction sintered Si_3N_4 than is the Norton material.

As seen in figure 4 the weight gain behavior of the A.M.E. reaction sintered Si_3N_4 compares favorably with the weight gain of the much higher density Ceradyne hot pressed Si_3N_4. This is somewhat surprising inasmuch as previous studies have reported much higher static oxidation weight gains for high porosity reaction sintered Si_3N_4 (Ref. 10) than for fully dense hot pressed Si_3N_4 (Ref. 7). The favorable behavior of A.M.E. material may well be at least partially caused by the high velocity gas stream. As illustrated in figure 19 a continuous SiO_2 scale does form which protects the underlying porous structure from continued rapid oxidation. The flow of SiO_2 augmented by the shearing forces of the gas stream no doubt contribute to the formation of this continuous protective scale.

The somewhat erratic behavior of both reaction sintered Si_3N_4 materials regarding pin groove failures is unfortunate, however, not totally unexpected for such relatively weak porous material. In light of the

preponderance of pin groove failures it appears that reaction sintered Si_3N_4 could have possibly reached the program goal of 100 cycles if an improved gripping technique were used. There, of course, is the suggestion of a possible thermal fatigue problem with the A.M.E. material, since two specimens failed in fatigue after 9 and 24 cycles and no specimen endured more than 49 cycles.

COATED TD Ni Cr

For comparison with the ceramics, a commercially aluminide coated 80 $^{w}/_{o}$ nickel -20 $^{w}/_{o}$ chromium alloy with 2 $^{w}/_{o}$ thoria dispersion for strengthening was exposed in the burner rig for 100 cycles. Although weight loss was high as indicated in table IV and two thermal fatigue cracks were evident on the leading edge at 20 cycles, exposure was continued to 100 cycles. The test specimen is shown in figure 20. The thermal fatigue cracks have developed into deep notches in the leading edge and the erosion of the leading edge is obvious. The metal specimen lost 41.5 mg/cm^2. Changes in weight for the ceramics surviving 100 cycles without damage were more than two orders of magnitude less than the 100 cycle weight loss for the coated TD Ni Cr. It is apparent that the coated dispersioned strengthened NiCr alloy is inferior to some of the better grades of SiC and Si_3N_4 in the behavior in this burner rig exposure.

SUMMARY OF RESULTS

In this investigation, specimens of 10 SiC and 5 Si_3N_4 materials supplied by different vendors were exposed in a Mach 1 gas velocity burner simulating a gas turbine engine environment. Cyclic tests were

conducted to a specimen temperature of 1200° C which resulted from exposure to the Mach 1 hot gas stream. Specimen behavior was judged on the basis of weight change, dimension losses, metallography, fluorescent penetrant inspection, x-ray diffraction analysis, failure mode and general appearance. Material test results are summarized below according to material classes.

HOT PRESSED SiC

One (Norton's) of the four materials tested survived the 100 cycles. It was characterized by a duplex structure of fine equiaxed grains. Weight change and microstructural observations indicated that this material formed a protective SiO_2 surface scale. The remaining three hot pressed SiC materials failed by thermal fatigue. One behaved very consistently with failures after 41 and 43 cycles. This material (A.C.E.) was fine grained, similar to Norton's but without the duplex grain size. Two materials behaved erratically with thermal fatigue failures occurring from 1 to 11 cycles in one material and from 1 to 48 cycles in another material. This erratic behavior and early failures are associated with heterogeneous microstructures of large grain size consisting of both equiax and tabular grains with large pores and some second phase remnants of sintering aids.

REACTION SINTERED SiC

Of the four reaction sintered SiC materials tested, one survived to the program target of 100 cycles. This material (Refel) had small equiaxed grains and a fully dense microstructure containing about 10% of finely distributed free silicon. As with three of the hot pressed

SiC materials, the remaining reaction sintered materials failed short of the program goal by thermal fatigue. Those materials that failed were characterized by rather inhomogeneous microstructures containing much larger microconstituents than the average 9 μm grain size of the successful material (Refel).

CVD SiC

CVC SiC failed between one and 52 cycles by fractures associated with the sample gripping technique. Judging from the small grain size, high density, and uniform microstructure CVD SiC would be expected to survive 100 cycles if an improved gripping technique were used.

HOT PRESSED Si_3N_4

All three test materials succeeded in reaching the 100 cycle target. No failures associated with the gripping pin groove were experienced. This, of course, would be expected with higher strength materials being more forgiving of design inadequacies. All hot pressed Si_3N_4 materials exhibited fully dense, fine grained, uniform microstructures. While oxidation behavior varied, apparently reflecting purity difference, all hot pressed Si_3N_4 materials tested were quite adequate in oxidation resistance.

REACTION SINTERED Si_3N_4

Both reaction sintered Si_3N_4 materials tested behaved similarly in that all failures originated at the gripping pin groove. This is not unexpected for such porous and comparatively weak materials. One material exhibited excessive oxidation apparently due to localized variations in the nitriding process.

COATED TD-NiCr

This metallic material, tested in order to give a direct comparison with the ceramic materials, did not experience any pin groove failures. This, of course, is due to its higher ductility. However, its oxidation and erosion resistance were far inferior to those of all the SiC and Si_3N_4 materials tested. The alloy also suffered thermal fatigue cracking early in the exposure.

CONCLUDING REMARKS

In this study various forms of SiC and Si_3N_4 were exposed to 1200° C, Mach 1 combustion products under thermal cycling conditions using a sample geometry that induced thermal stresses. Several forms of both SiC and Si_3N_4 were identified that are fully capable of withstanding over 100 cycles under the severe environmental conditions of this exposure. These materials are therefore judged to be of adequate quality to justify further material and design developments that could ultimately lead to the use of these materials in advanced aircraft gas turbine engines.

This study identified three types of materials that met the 100 cycle goal and have potential for continued improvement; these are, hot pressed Si_3N_4, Norton's hot pressed SiC, and Refel reaction sintered SiC.

The microstructural features associated with successful survival in this simulated gas turbine environment are generally those characteristic of a high quality structural ceramic product. They are high density, fine grain size, small size of microconstituents and flaws, and a homogeneous microstructure. Conversely, features associated with

early failures are: low density, large grain size, large pores and second phase microconstituents, and non-uniform microstructures.

Specific conclusions regarding particular materials and material characteristics are as follows:

1. A duplex, but fine grain size distribution as exemplified by Norton's hot pressed SiC contributes to high strength and resistance to thermal fatigue and gripping stresses in the simulated gas turbine environment.
2. The presence of free silicon in SiC, so long as it is finely distributed and accompanied by a fine grain size SiC matrix as exemplified by Refel does not lead to any degradation in performance as compared to hot pressed SiC (Norton's) under the conditions of these tests.
3. CVD-SiC has promise and judging from its microstructural features there is no obvious reason why its eventual performance in a gas turbine environment could not match or exceed that of hot pressed SiC.
4. While both SiC and Si_3N_4 form SiO_2 upon oxidation, results of this study suggest the SiO_2 on SiC is more viscous than that formed on Si_3N_4 and therefore resists viscous flow and offers better protection against oxidation. This apparently reflects differences in purity levels of specific elements in the several materials available for tests in this study.
5. Reaction sintered Si_3N_4, although porous and comparatively weak could apparently withstand the rigors of thermal cycling in a high velocity gas stream of a gas turbine engine. In

this study, however, this lower strength material was particularly prone to grip failures, thus, components to be made of reaction sintered Si_3N_4 will require excellent gripping designs to accommodate lower strength.

A general conclusion that emerges from this and previous work is that once a ceramic material possesses the necessary combination of strength, thermal conductivity, elastic modulus, Poissons ratio, and thermal expansion in order to survive thermal shock failure; then the mechanical properties, strength and elastic modulus become paramount in determining the materials ability to survive in the gas turbine environment. That is to say, if a ceramic material can resist the severe transients associated with one cycle of gas turbine operation, i.e., start-up and shut-down, then the most likely failure modes are primarily mechanical resulting from aerodynamic loading, containment (gripping) loads, thermal fatigue, and mechanical impact. Resistance to such mechanical failure is, of course, favored by high strength and low elastic modulus accompanied by some degree of toughness. Thus, the higher the ratio of strength to elastic modulus and the more reliable (reproducible) these mechanical properties are, the more likely the material can withstand operational stresses and the less it is dependent on critical designs to accommodate its brittleness. Therefore, continued efforts should be devoted to SiC and Si_3N_4 in order to increase strength, lower elastic modulus, and impart some degree of toughness.

TABLE I. - VENDOR REPORTED PROPERTIES FOR SiC AND Si_3N_4 MATERIALS

Material Category and Vendor	Billet Dimensions cm	Density g/cm^3	Porosity v/o	Purity Element, w/o	Room Temperature			
					Bend Strength		Modulus of Elasticity	
					MN/m^2	psi	MN/m^2	psi
Hot Pressed SiC								
Norton	10.2x10.2x3.0	> 3.17	--	Al-1, W-4, Fe-0.1[10]	730	[5] $106x10^3$	$440x10^3$	[5] $64x10^6$
[a]A.C.E.	10.7x5.1x2.8	3.12	--	--	540	[18] $79x10^3$	--	--
AVCO	15.2x15.2x0.64	3.13	--	--	--	--	--	--
Ceradyne	15.2x15.2x2.5	3.19	--	--	--	--	--	--
Reaction Sintered SiC								
Norton-Low Fired	11.4x11.4x0.79	2.67	18	< 1% Impurity[2]	120	[2] $18x10^3$	$190x10^3$	$28x10^6$
Norton-High Fired	11.4x11.4x0.79	2.70	18	< 1% Impurity[2]	100	[2] $15x10^3$	$210x10^3$	$30x10^6$
[b]U.K.A.E.A.-Refel	12.7x10.2x0.97	3.12	<0.1	10% Free Si[12]	410	[12] $60x10^3$	$410x10^3$	[12] $60x10^6$
Carborundum-KT	11.4x11.4x0.79	3.10	0	9% Free Si	160	$23x10^3$	$390x10^3$	$56x10^6$
[c]S.F.L. Si-SiC-C	12.7x12.7x0.97	2.71	--	--	--	--	--	--
Chemical Vapor Deposited SiC								
[d]E.R.C.	*	3.20	0	--	--	--	--	--
Hot Pressed Si_3N_4								
Norton HS-130	15.2x15.2x3.0	> 3.17	--	Mg-0.6, Fe-0.5, W-2[10]	830	$120x10^3$	$310x10^3$	$45x10^6$
Ceradyne	15.2x15.2x2.9	> 3.17	--	--	830	$120x10^3$	$310x10^3$	$45x10^6$
AVCO	22.6x22.6x0.97	3.16	--	--	--	--	--	--
Reaction Sintered Si_3N_4								
Norton NC-350	*	2.40	--	--	240	$35x10^3$	$160x10^3$	$23x10^6$
[e]A.M.E.	11.4x11.4x0.97	2.50	--	--	180	$26x10^3$	$150x10^3$	$22x10^6$

[a] Alfred Ceramic Enterprises
[b] United Kingdom Atomic Energy Authority
[c] San Fernando Laboratories
[d] Energy Research Corporation
[e] Advanced Materials Engineering

( ) Reference Number

* Specimens provided by vendor machined to dimensions of Figure 1

TABLE II. - MACH 1 BURNER CONDITIONS FOR EVALUATION OF SiC AND Si_3N_4 MATERIALS

[Specimen Test Cycle: 1 Hour at 1200° C; 5 Minute Still Air Cool]

Burner Gas Temperature, ° C	1540
Burner Nozzle Diameter, cm (in.)	5.1 (2.0)
Air to Fuel Ratio	20 : 1
Burner Air Flow, kg/sec (lbm/sec)	0.4 to 0.5 (0.9 to 1.0)
Burner Pressure, MN/m^2 (psia)	0.23 (33)

TABLE III. - SUMMARY OF TEST RESULTS FOR SiC AND Si_3N_4 MATERIALS EVALUATED AT 1200° C IN A MACH 1 SIMULATED GAS TURBINE ENVIRONMENT

Material Category and Vendor	Cycles Completed Before Thermal Fatigue Failure	Other Reasons for Test Termination
Hot Pressed SiC		
Norton	No Failure After 100 Cy.	---
[a]A.C.E.	41, 43	---
AVCO	1, 1, 3, 47	---
Ceradyne	1, 1, 1, 2, 11	---
Reaction Sintered SiC		
Norton-Low Fired	22	Failure in pin groove in 26th cy. due to loosening in holder.
Norton-High Fired	0, 1, 1, 1, 1	---
[b]U.K.A.E.A.-Refel	No Failure After 100 Cy.	Failure in pin groove in 89th cy. due to loosening in holder.
Carborundum-KT	1, 1, 1, 1, 1, 10	---
[c]S.F.L. Si-SiC-C	---	Excessive wt. loss 1 cy.
Chemical Vapor Deposited SiC		
[d]E.R.C.	---	Failures in pin groove after 1, 9, 29, and 52 cy. due to loosening in holder.
Hot Pressed Si_3N_4		
Norton HS-130	No Failure After 100 Cy.	---
Ceradyne	No Failure After 100 Cy.	---
AVCO	No Failure After 100 Cy.	---
Reaction Sintered Si_3N_4		
Norton NC-350	---	Failures in pin groove after 54 and 92 cy. due to loosening in holder.
[e]A.M.E.	9, 24	Failures in pin groove after 7, 9, 10, 10 and 49 cy. due to loosening in holder.

[a] Alfred Ceramic Enterprises
[b] United Kingdom Atomic Energy Authority
[c] San Fernando Laboratories
[d] Energy Research Corporation
[e] Advanced Materials Engineering

TABLE IV. - SPECIFIC WEIGHT CHANGES AND DIMENSIONAL LOSSES FOR TEST MATERIALS RESULTING FROM CYCLIC EXPOSURE AT 1200° C IN MACH 1 SIMULATED GAS TURBINE ENVIRONMENT. CYCLE: 1 HR. AT 1200° C, 5 MIN. STILL AIR COOL.

Material Category and Vendor	*Specific Weight Change, mg/cm^2					Dimensional Loss After 100 Cy., μm	
	20 Cy.	40 Cy.	60 Cy.	80 Cy.	100 Cy.	Breadth	Thickness
Hot Pressed SiC							
Norton	+.10	+.21	+.12	+.16	+.18	14	4
[a]A.C.E.	+.22	+.04					
AVCO	+.29	+.27					
Ceradyne	‡						
Reaction Sintered SiC							
Norton-Low Fired	+17.4						
Norton-High Fired	‡						
[b]U.K.A.E.A.-Refel	+.04/+.09	+.12/+.21	+.10/+.25	+.14/+.23	+.16	17	0
Carborundum-KT	‡						
[c]S.F.L. Si-SiC-C	‡						
Chemical Vapor Deposited SiC							
[d]E.R.C.	+.10	Base Chipped				5 (52 cy.)	3 (52 cy.)
Hot Pressed Si_3N_4							
Norton HS-130	+.08/+.04	+.01/+.08	-.08/+.08	-.21/+.04	-.50/-.01	3	3
Ceradyne	+.42/+.18	+.41/+.22	+.71/+.26	+.41/+.31	+.20/+.42	25	12
AVCO	+.31	+.15	+.33	+.20	+.02	20	7
Reaction Sintered Si_3N_4							
Norton NC-350	+3.69	+5.48	+5.80	+6.59		Not Measureable Due to Trailing Edge Damage	11 (92 cy.)
[e]A.M.E.	+.47 (17 cy.)	+.57					
Commercially Coated TD NiCr	-3.59	-13.0	-20.8	-29.3	-41.5		

[a] Alfred Ceramic Enterprises
[b] United Kingdom Atomic Energy Authority
[c] San Fernando Laboratories
[d] Energy Research Corporation
[e] Advanced Materials Engineering

* Second Value for Duplicate Specimen

‡ Did Not Survive to 20 Cycles

SUMMARY

Specimens which incorporated a simulated leading edge of an airfoil of 10 varieties of silicon carbide (SiC) and 5 varieties of silicon nitride (Si_3N_4) were exposed in a high gas velocity burner simulating a gas turbine engine environment. Cyclic tests were conducted to a maximum specimen temperature of 1200° C which resulted from exposure to a Mach 1 hot gas stream. Each cycle consisted of 1 hour at 1200° C followed by 5 minutes cooling to near room temperature. SiC and Si_3N_4 evaluations and comparisons were based on weight change, inspection for cracks, dimensional loss, metallography, x-ray diffraction, failure mode, and appearance.

One hot pressed form of SiC, one reaction sintered SiC and three hot pressed forms of Si_3N_4 survived 100 hours of cyclic exposure at a specimen temperature of 1200° C. Specimen weight changes and material losses were slight and the specimens were not cracked.

Other SiC and Si_3N_4 forms failed in thermal fatigue. These materials were characterized by tabular grain structures and second phases or by low density, coarse grained, non-homogeneous microstructures.

Experimental difficulties prevented certain materials from being definitively evaluated. Loosening in the specimen holder prevented the completion of tests on chemical vapor deposited SiC and reaction sintered Si_3N_4. It is felt that both of these material could survive the 100 cycle exposure goal if improved gripping techniques were used.

REFERENCES

1. Sanders, William A., and Probst, Hubert B., "Evaluation of Oxidation Resistant Nonmetallic Materials at 1204° C (2200° F) in a Mach 1 Burner," National Aeronautics and Space Administration Report TN D-6890, August 1972.

2. Alliegro, R. A., and Coes, S. H., "Reaction Bonded Silicon Carbide and Silicon Nitride for Gas Turbine Applications," American Society of Mechanical Engineers Paper 72-GT-20, March 1972.

3. McLean, Arthur F., Fisher, Eugene A., and Harrison, Don E., "Brittle Materials Design, High Temperature Gas Turbine," Ford Motor Company. Army Materials and Mechanics Research Center Report AMMRC-CTR-72-3, March 1972.

4. McLean, Arthur F., "Ceramics in Automotive Gas Turbines," Bull. Am. Ceram. Soc., 52, no. 5 (May 1973), 464-466, 482.

5. Alliegro, R. A., Comp., "Silicon Nitride and Silicon Carbide for High Temperature Engineering Applications," Norton Company, Industrial Ceramics Division, July 1972.

6. Anon., "2500 F Target for 30-Mw Ceramics Test Turbine," Gas Turbine World, 2, no. 3 (August 1972), 34-40.

7. McLean, Arthur F., Fisher, Eugene A., and Bratton, Raymond J., "Brittle Materials Design, High Temperature Gas Turbine," Ford Motor Company. Army Materials and Mechanics Research Center Report AMMRC-CTR-72-19, September 1972.

8. deBiasi, Victor, "2500° F Target for Vehicular Ceramic Turbine," Gas Turbine World, 2, no. 4 (October-November 1972), 12-19.

9. Alliegro, R. A., and Torti, M. L., "Ceramics - Key to the "Hot" Turbine," Gas Turbine Int. (January-February 1973), 30-36.

10. McLean, Arthur F., Fisher, Eugene A., and Bratton, Raymond J., "Brittle Materials Design, High Temperature Gas Turbine," Ford Motor Company. Army Materials and Mechanics Research Center Report AMMRC-CTR-73-9, March 1973.

11. Caws, R. B., Graham, R. P., and Stoddart, D. E., "Silicon Nitride Materials for Gas Turbine Components," American Society of Mechanical Engineers Paper 73-GT-47, April 1973.

12. Forrest, C. W., Kennedy, P., and Shennan, J. V., "The Fabrication and Properties of Self-Bonded Silicon Carbide Bodies," United Kingdom Atomic Energy Authority Report TRG Report 2053(S), July 1970.

13. Private Communication with Mr. Andrew M. Cecka, San Fernando Laboratories, Pacoima, California.

14. Anon., Carborundum Company Bulletin, Form No. A-1716-A.

15. Kern, E. L., Hamill, D. W., and Jacobson, K. A., "Fabricating Parts by Chemical Vapor Deposition," Proceedings of the 14th National Symposium and Exposition, Society of Aerospace Material and Process Engineers, Cocoa Beach, Florida, November 1968, Section II-2B-3.

16. Johnston, James R., and Ashbrook, Richard L., "Oxidation and Thermal Fatigue Cracking of Nickel and Cobalt-Base Alloys in a High Velocity Gas Stream," National Aeronautics and Space Administration Report TN D-5376, August 1969.

17. Lange, F. F., and Terwilliger, G. R., "Fabrication and Properties of Silicon Compounds," Westinghouse Electric Corporation. Naval Air Systems Command, Report 72-9D2-SERAM-R1, January 1972.

18. Platts, D. R., Kirchner, H. P., and Gruver, R. M., "Strengthening of Oxidation Resistant Materials for Gas Turbine Applications," Ceramic Finishing Company. NASA Lewis Research Center Report NASA CR-121002, September 1972.

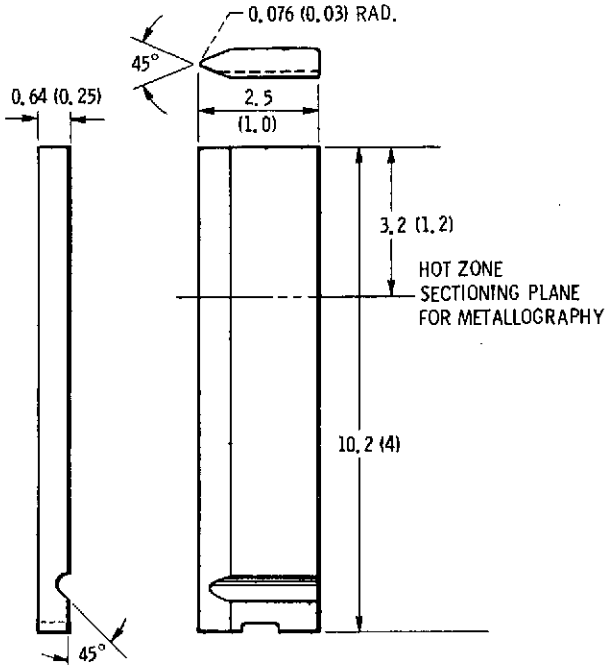

Figure 1. - Specimen used in high-gas-velocity oxidation tests. (Dimensions are in cm (in.).)

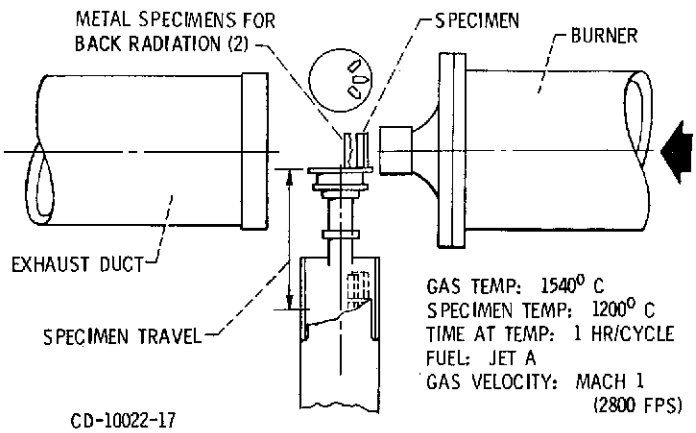

Figure 2. - Burner rig for simulated gas turbine environment.

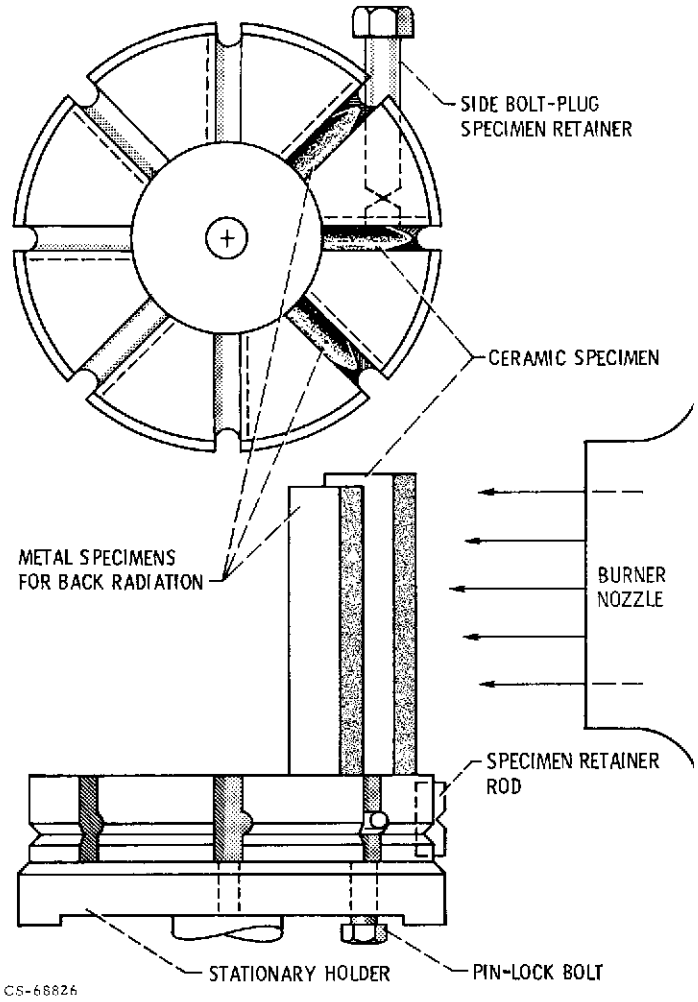

Figure 3. - Schematic of specimen-holder-nozzle arrangement for exposing test specimen.

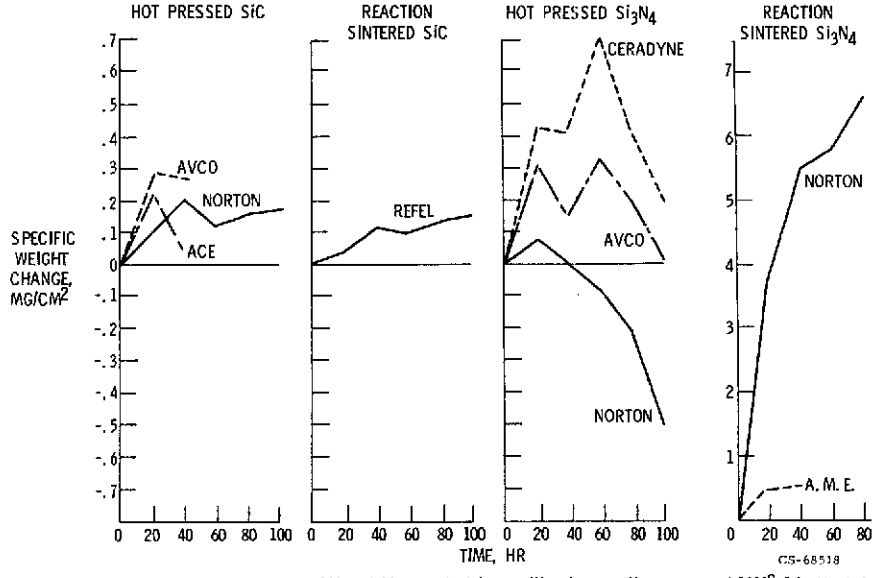

Figure 4. - Specific weight change for SiC and Si_3N_4 materials resulting from cyclic exposure at 1200° C in Mach 1 simulated gas turbine environment cycle; 1 hour at 1200° C, 5 minute still air cool.

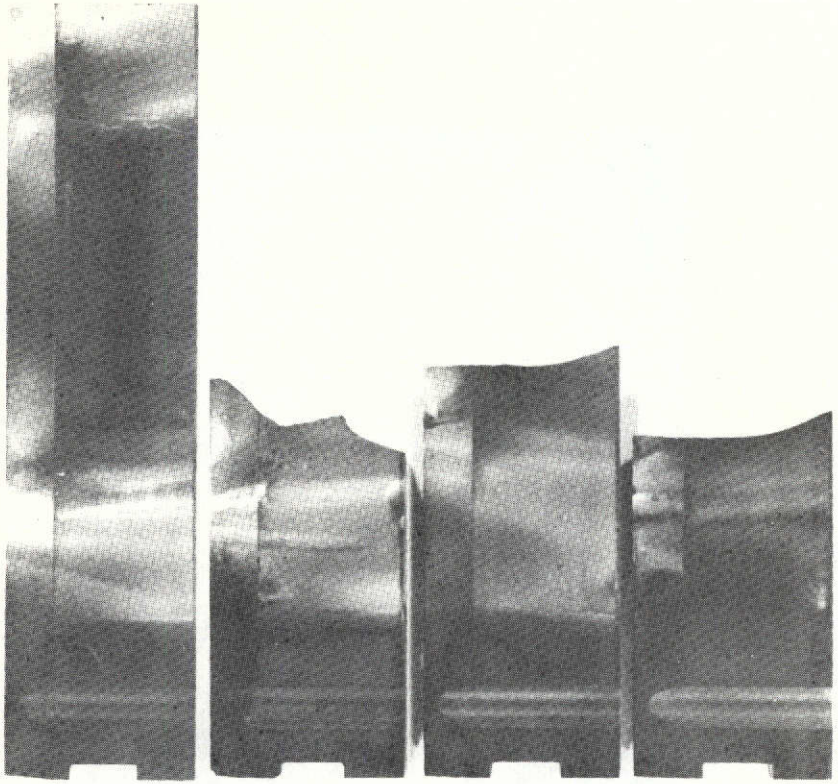

NORTON, 100CYCLES. NO DAMAGE OBSERVED.

A.C.E., THERMAL FATIGUE FAILURE AFTER 43 CYCLES.

AVCO, THERMAL FATIGUE FAILURE AFTER 47 CYCLES.

CERADYNE, THERMAL FATIGUE FAILURE AFTER 11 CYCLES.

Figure 5. - Hot pressed SiC specimens after cyclic exposure in Mach 1 simulated gas turbine environment. Cycle: 1 hour at 1200° C; 5 minute still air cool.

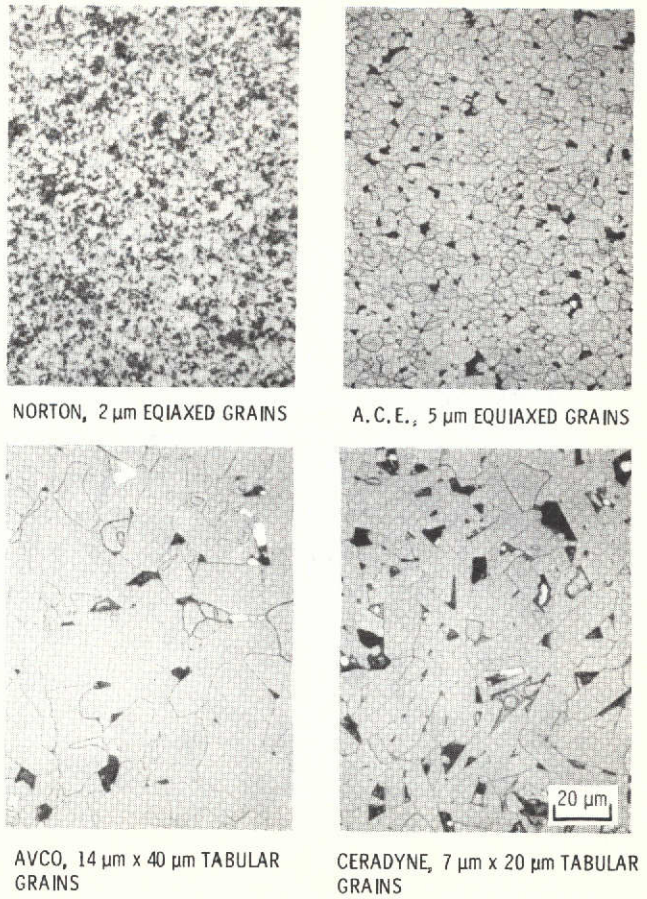

NORTON, 2 µm EQIAXED GRAINS

A.C.E., 5 µm EQUIAXED GRAINS

AVCO, 14 µm x 40 µm TABULAR GRAINS

CERADYNE, 7 µm x 20 µm TABULAR GRAINS

Figure 6. - Microstructures of as-received hot pressed SiC materials. Etched, X750.

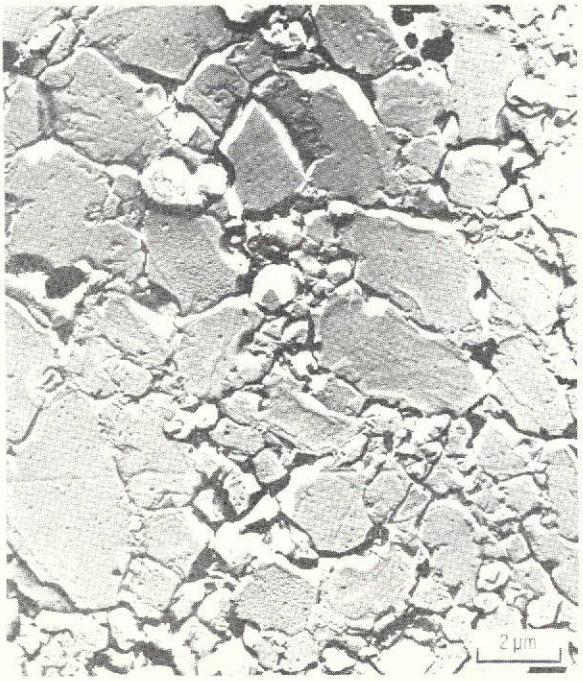

Figure 7. - Electron micrograph of as-received Norton hot pressed SiC. Etched, X11 000.

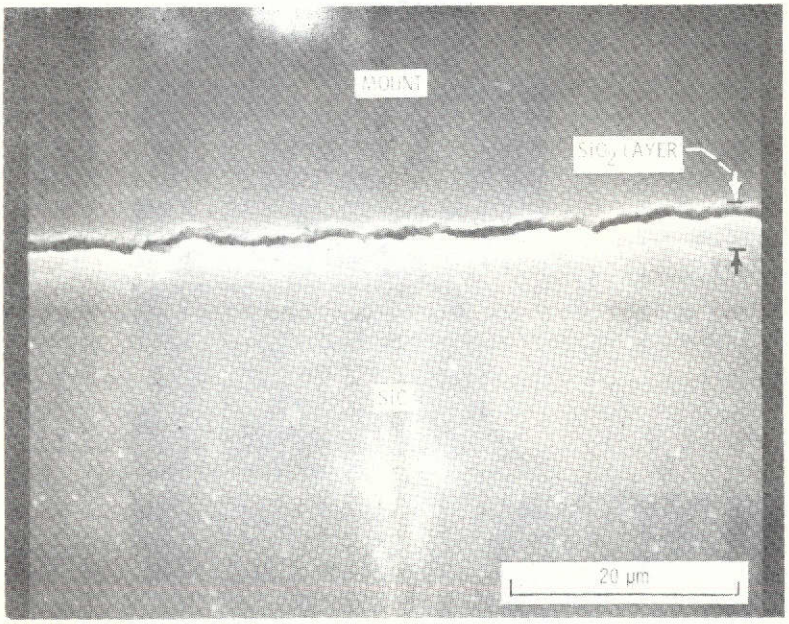

Figure 8. - Scanning electron micrograph of Norton hot pressed SiC specimen hot zone cross section after 100 cycle specimen exposure. Cycle: 1 hour at 1200° C; 5 minute still air cool. X1500.

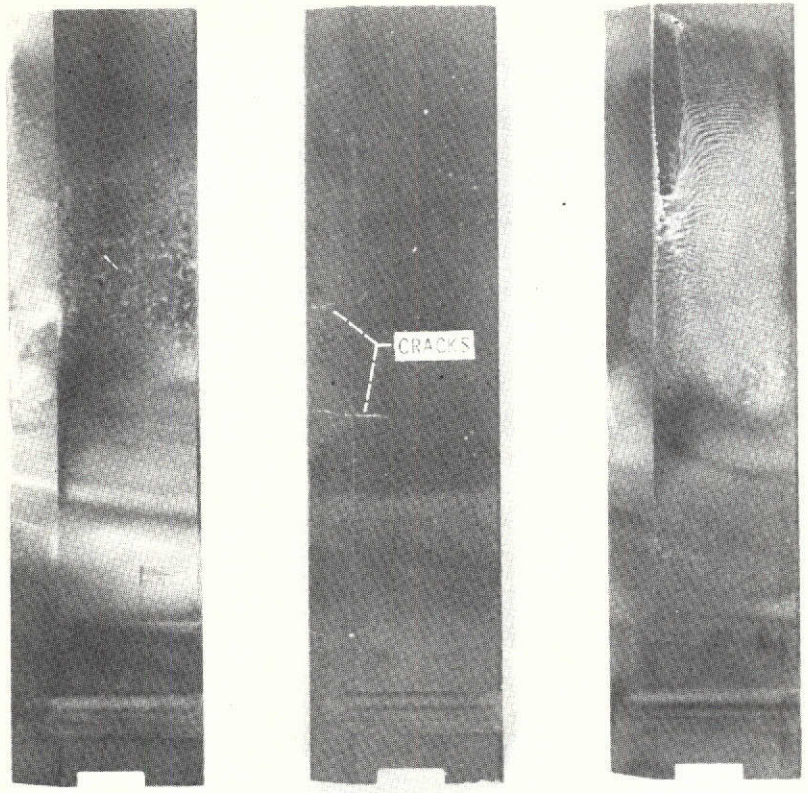

REFEL, 100 CYCLES.
NO DAMAGE OBSERVED.

KT, THERMAL FATIGUE
CRACKS AFTER 10
CYCLES.

NORTON LOW-FIRED,
20 CYCLES.
SILICA FLOW LINES.

Figure 9. - Reaction sintered SiC specimens after cyclic exposure in Mach 1 simulated gas turbine environment. Cycle: 1 hour at 1200° C; 5 minute still air cool.

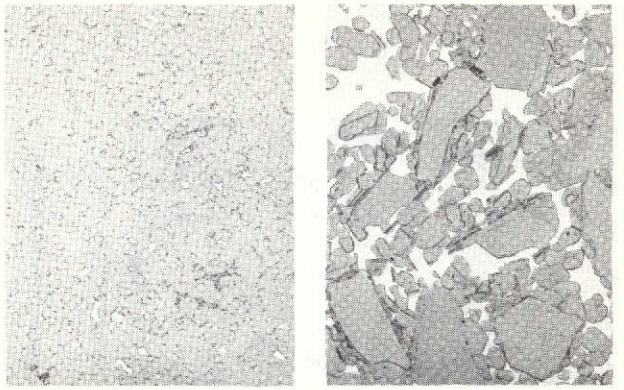

REFEL, 9 μm EQUIAXED GRAINS

KT, 40 μm EQUIAXED GRAINS

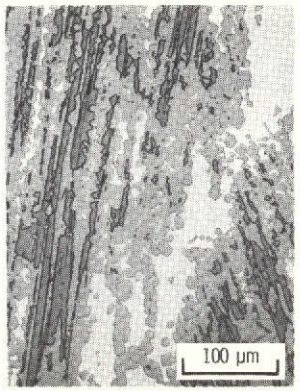

Si-SiC-C - STRIATED

Figure 10. - Microstructures of as-received reaction sintered SiC materials. Etched, X250.

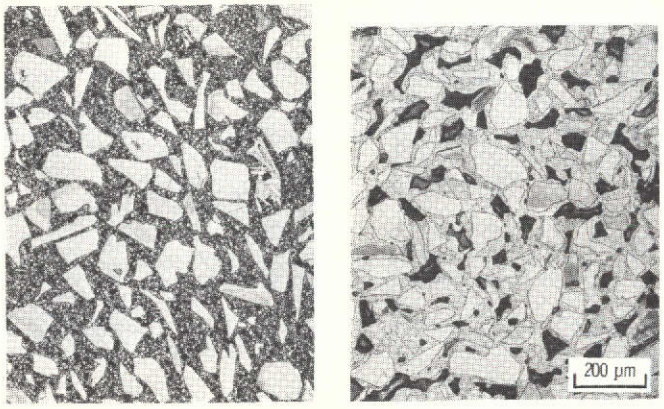

NORTON LOW FIRED SiC
DUPLEX GRAIN SIZE: 100 µm, 4 µm

NORTON HIGH FIRED SiC

Figure 11. - Microstructures of as-received reaction sintered (recrystallized) SiC materials. Etched, X100.

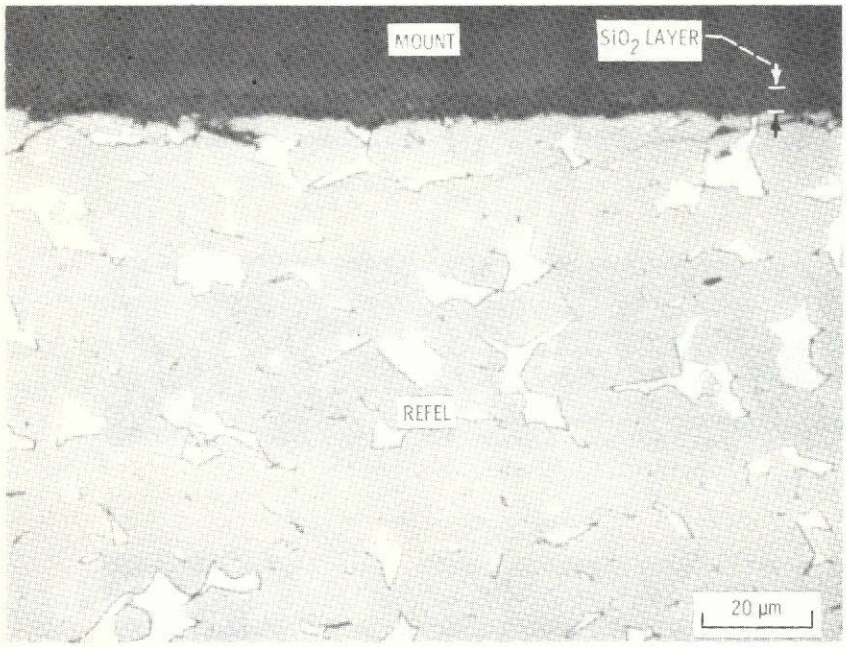

Figure 12. - Light micrograph of REFEL reaction sintered SiC specimen hot zone cross section after 100 cycle specimen exposure. Cycle: 1 hour at 1200° C; 5 minute still air cool. Etched, X750.

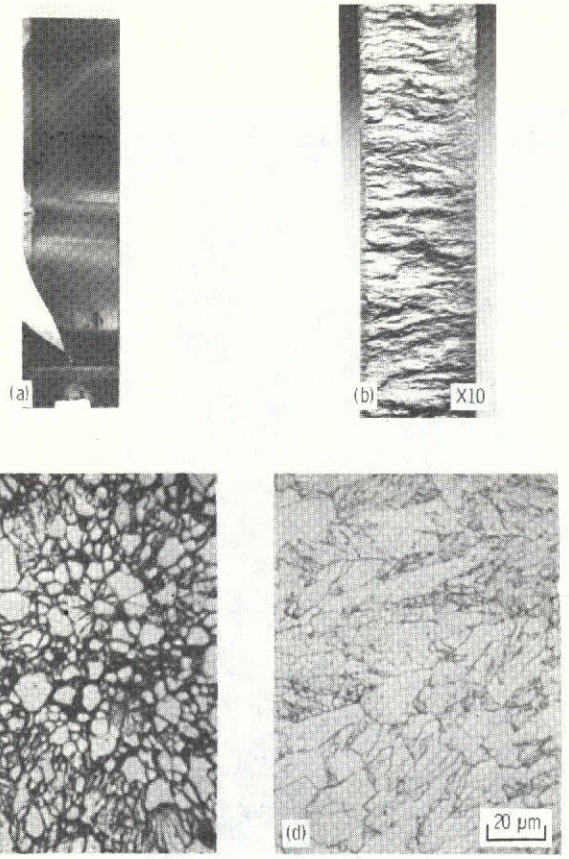

Figure 13. - CVD SiC material: (a) failed specimen, loosened in holder; (b) fracture face columnar structure, X10; (c) as-received microstructure, deposition plane, etched, X750; and (d) as-received microstructure, plane perpendicular to deposition plane, etched, X750.

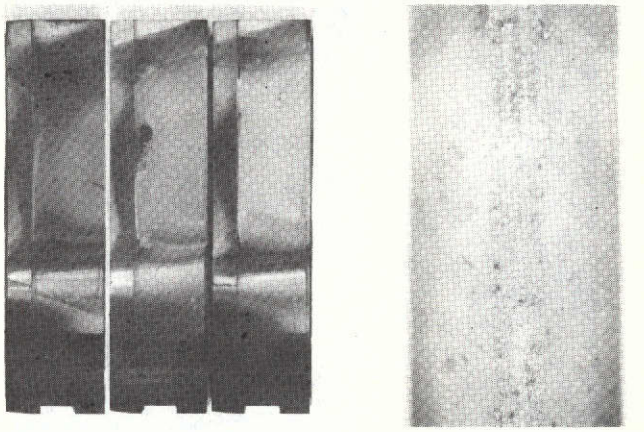

Figure 14. - (a) Hot pressed Si_3N_4 specimens undamaged after 100 cycle exposure in Mach 1 simulated gas turbine environment. Cycle: 1 hour at 1200° C, 5 minute still air cool. (b) Hot zone leading edge of Avco Si_3N_4 specimen representative of 100 cycle exposure condition for Ceradyne and Avco Si_3N_4 specimens showing silica flow lines, X10.

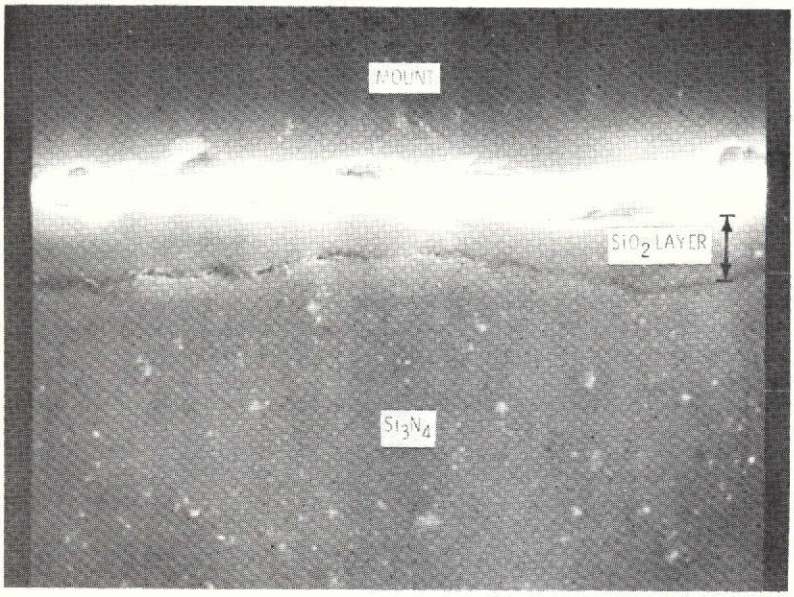

NORTON

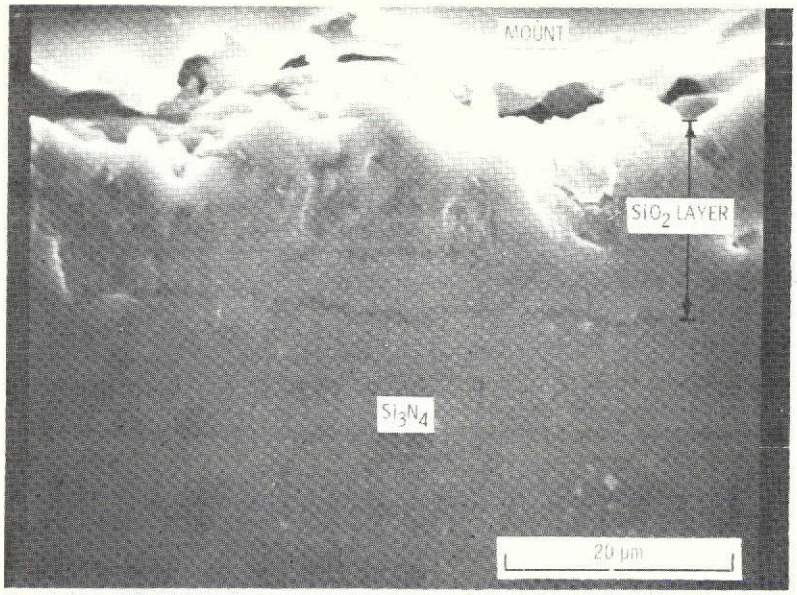

AVCO - ALSO REPRESENTATIVE OF CERADYNE

Figure 15. - Scanning electron micrographs of hot pressed Si_3N_4 specimen hot zone cross sections after 100 cycle specimen exposure. Cycle: 1 hour at 1200^0 C; 5 minute still air cool. X1500.

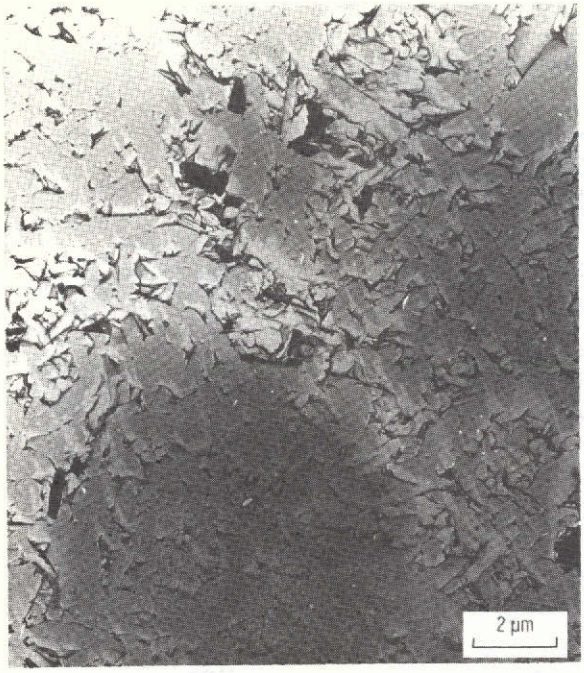

Figure 16. - Electron micrograph of as-received Norton hot pressed Si_3N_4. Etched X11 000.

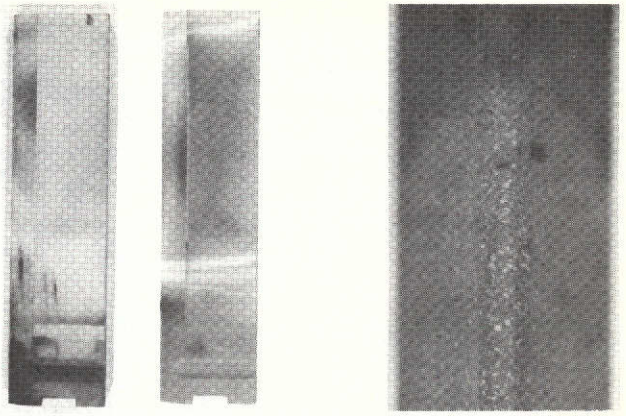

NORTON, 80 CYCLE CONDITION

A.M.E., 40 CYCLE CONDITION

(a)

(b) A.M.E., HOT ZONE LEADING EDGE AFTER 20 CYCLES, X10.

Figure 17. - (a) Reaction sintered Si_3N_4 specimens after cyclic exposure in Mach 1 simulated gas turbine environment. Cycle: 1 hour at 1200° C, 5 minute still air cool. (b) A.M.E. reaction sintered Si_3N_4 specimen hot zone leading edge after 20 cycles showing silica flow lines.

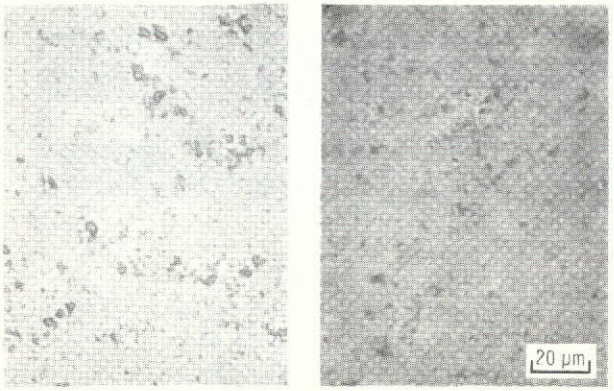

(a) NORTON (LEFT) AND A.M.E.

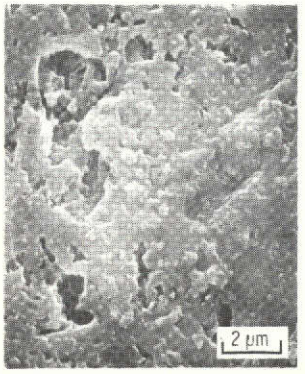

(b) A.M.E.

Figure 18. - (a) Microstructures of as-received reaction sintered Si_3N_4 materials, unetched, X750. (b) Scanning electron micrograph of as-received A.M.E. reaction sintered Si_3N_4, 10 000.

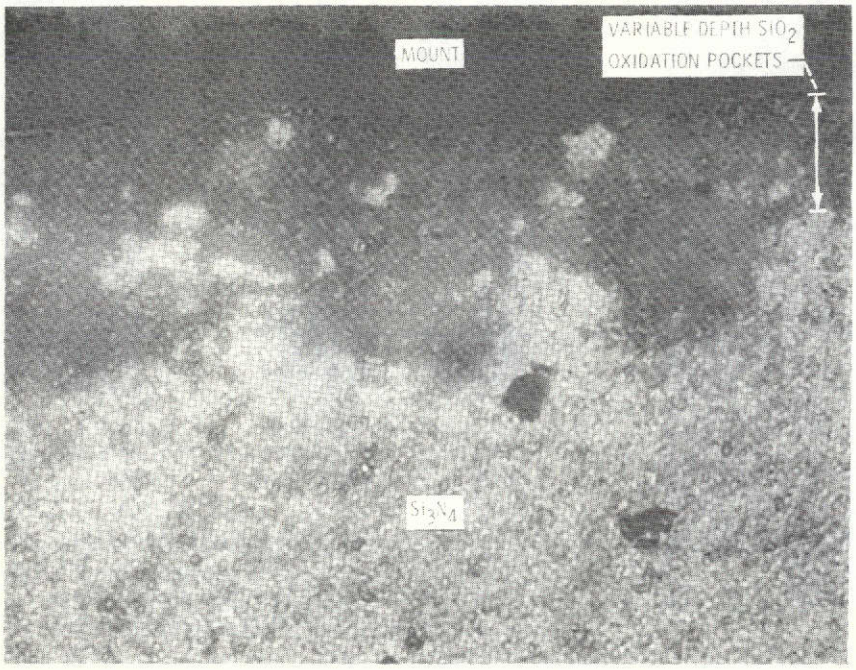

WHITE SIDE

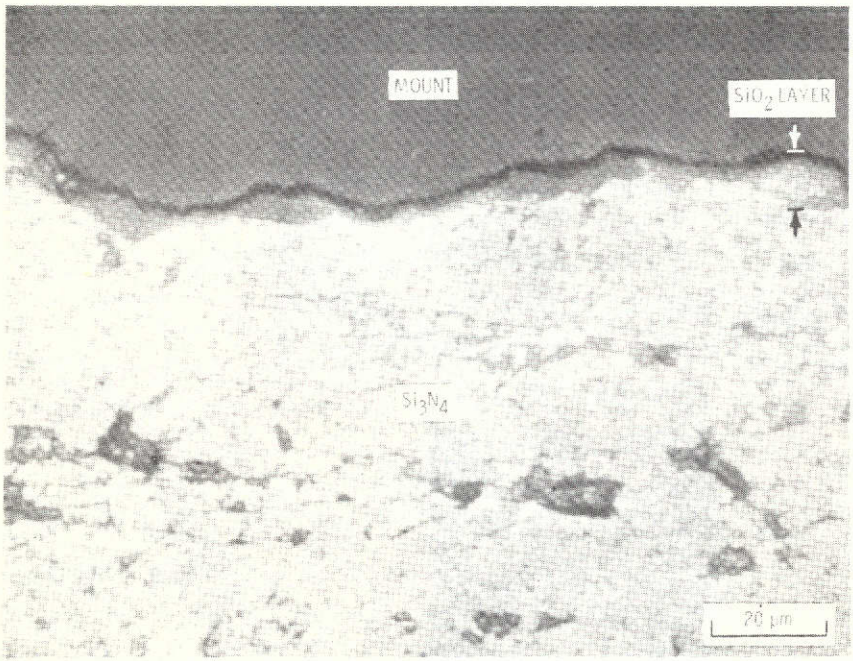

GRAY SIDE

Figure 19. - Microstructure comparison of opposite sides of Norton reaction sintered Si_3N_4 specimen hot zone cross section after 92 cycles exposure. Cycle: 1 hour at 1200° C; 5 minute still air cool. Unetched, X750.

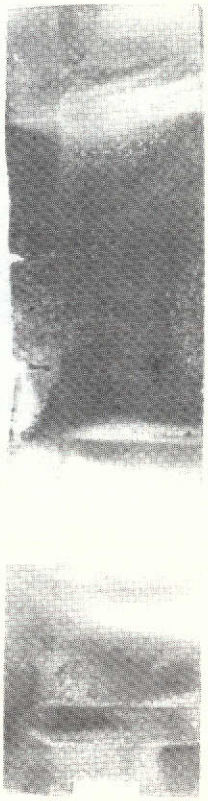

Figure 20. - Commercially coated TDNiCr specimen after 100 cycle exposure in Mach 1 simulated gas turbine environment. Cycle: 1 hr at 1200° C, 5 minute still air cool.